

# System-Level Optical Interface Modeling for Microsystems

Timothy P. Kurzweg<sup>\*</sup>, Ankur S. Sharma<sup>\*</sup>, Shubham K. Bhat<sup>\*</sup>,  
Steven P. Levitan<sup>\*\*</sup>, and Donald M. Chiarulli<sup>\*\*</sup>

<sup>\*</sup>Drexel University, Department of Electrical and Computer Engineering,  
Philadelphia, PA 19104, kurzweg@ece.drexel.edu

<sup>\*\*</sup>University of Pittsburgh, Departments of Electrical Engineering and Computer Science,  
Pittsburgh, PA 15261

## ABSTRACT

In this paper, we present an accurate and computationally efficient system-level optical propagation technique suitable for the modeling of optical interfaces. Our technique is based on extensions to the angular spectrum technique used to solve the Rayleigh-Sommerfeld formulation. By using a FFT, the angular spectrum technique is efficient and suitable for system-level modeling of the complete system. To support the reflection and transmission at optical interfaces, we implement a semi-vector technique, taking into account the polarization of the optical wavefront. The polarization is used to determine the reflection and transmission coefficients through the use of Berreman's 4x4 matrix. Solutions are provided for typical TE and TM waves, however, wavefronts with arbitrary linear polarization are also supported. In this paper, we present a system-level simulation of a Silicon on Sapphire (SOS) interface.

**Keywords:** angular spectrum, semi-vector, Fresnel coefficients, FDTD, system-level simulation.

## 1 INTRODUCTION

Current optical systems are becoming smaller with rapid developments in the field of device fabrication. [1]. In addition, optical coatings and thin films are being used advantageously to increase the performance of optical microsystems. As optical devices approach the size of optical wavelengths, full vector solutions, such as the Finite Difference Time Domain (FDTD) technique, are required for accurate solutions. However, the distance of propagation computationally limits the FDTD approach, as distances on the order of tens to hundreds of wavelengths require excess solutions for the electromagnetic boundary conditions [1]. To overcome this costly computation, a scalar approach is typically used to solve for propagation of distances larger than the wavelength of light. In previous work, we have shown the use of a scalar approach for accurate and efficient modeling of systems using the angular spectrum technique, used to solve the Rayleigh-Sommerfeld formulation [3]. The limiting condition on scalar techniques is the distance of propagation, which must

be greater than the wavelength of operation. Therefore, scalar method cannot be used for optical modeling at optical interfaces due to its inherent drawback to account for the reflected and transmitted rays. Typically, a full-vector approach is used to solve for the reflected and transmitted wavefronts, however, as discussed earlier, this technique is computationally inefficient for full system simulation. In this paper, we present a semi-vector scalar solution used to model optical interfaces accurately and efficiently. Our system-level modeling requires a two-step approach: the angular spectrum technique is used to solve for propagation, and a semi-vector approach is used to solve for the optical interfaces.

## 2 TECHNIQUE

In this section, we present our semi-vector modeling of an optical interface. We first show the angular spectrum technique, followed by our extension for the reflection and transmission waves.

### 2.1 Angular Spectrum Technique

The angular spectrum technique, used to solve the Rayleigh-Sommerfeld formulation, decomposes a complex wavefront into a set of plane waves through a Fourier transform. Each plane wave is multiplied by the medium transfer function and recombined into a propagated complex wave by taking the inverse Fourier transform. We next present brief details on the technique.

Consider the propagation of a monochromatic optical wave of wavelength  $\lambda$  and complex amplitude  $U(x,y,z)$  in free space between the planes  $z = 0$  and  $z = d$ , called the aperture and observation planes respectively.  $d$  denotes the distance between the two planes in the  $z$  direction. Let us regard  $f(x,y) = U(x,y,0)$  as the complex amplitude at the aperture plane and  $g(x,y) = U(x,y,d)$  as the complex amplitude of the observation plane. These planes are shown in Figure 1.

The Fourier transform of the input wave,  $A(v_x, v_y, 0)$ , decomposes the complex optical wavefront into plane waves defined by the spatial frequencies  $v_x$  and  $v_y$ . The Fourier Transform is shown in Equation (1).

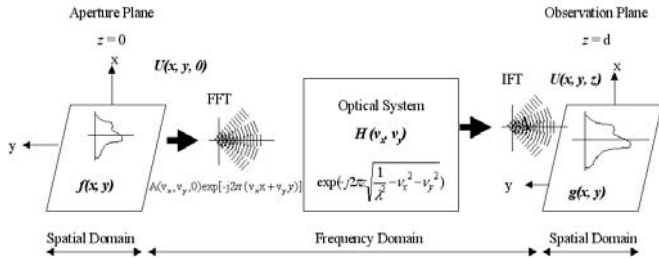


Figure 1: Angular spectrum method

$$A(v_x, v_y, 0) = \iint U(x, y, 0) \exp[-j2\pi(v_x x + v_y y)] \delta x \delta y \quad \dots(1)$$

The  $\exp\{-j2\pi(v_x x + v_y y)\}$  term represents the plane waves propagating with different angles related to the spatial frequencies:  $\theta_x = \sin^{-1}(\lambda v_x)$  and  $\theta_y = \sin^{-1}(\lambda v_y)$ . This is also graphically shown in Figure 1.

The product of the free space/propagation transfer function and the wave function in the frequency domain, describes the position of each of the plane waves after propagation. The plane waves are transformed back into the spatial domain using the inverse Fourier transform seen below:

$$U(x, y, z) = \iint A(v_x, v_y, 0) \exp[-j2\pi(v_x x + v_y y)] \exp(-jk_z z) \delta v_x \delta v_y \quad \dots(2)$$

In this equation  $k_z = 2\pi(1/\lambda^2 - v_x^2 - v_y^2)^{1/2}$ . Further details can be found in [3].

## 2.2 Angular Spectrum Extension for Reflected and Transmitted waves

To support reflection and transmission at the optical interface, we must find coefficients for the reflected and transmitted waves. This is achieved in three steps, which are applied to each plane wave in the frequency domain.

1. Calculate the spatial frequencies and transmission angles ( $v_{tx}, v_{ty}, \theta_{tx}, \theta_{ty}$ ) using Snell's law.
2. Determine the reflection and transmission coefficients  $R(v_x, v_y)$  and  $T(v_x, v_y)$ .
3. Multiply  $R(v_x, v_y)$  and  $T(v_x, v_y)$  to obtain the reflected and transmitted waves respectively.

Details are provided in the following sections.

### 2.2.1 Calculation of $v_{ty}, v_{tx}, \theta_{tx}, \theta_{ty}$

At the boundary between two planar isotropic media, the incident plane wave in the frequency domain is decomposed into a reflected and a transmitted ray, as shown in Figure 2.

In order to calculate the reflection and transmission coefficients we first need to determine the reflected,  $\theta_{rx}$  and  $\theta_{ry}$ , and transmitted angles,  $\theta_{tx}$  and  $\theta_{ty}$ , which are related to the spatial frequencies for each plane wave in both the x and y directions. By applying Snell's law we calculate the transmitted angles with the following relations:

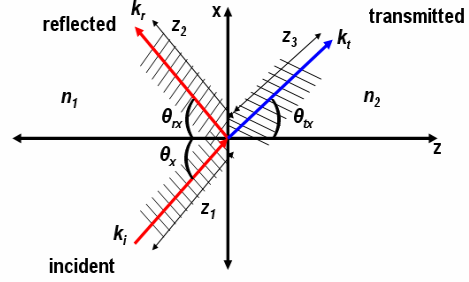


Figure 2: Reflection and transmission at the boundary between two planar isotropic media.

$$\theta_{rx} = \arcsin(n_i / n_t \sin \theta_x) \quad \dots(3)$$

$$\theta_{ry} = \arcsin(n_i / n_t \sin \theta_y) \quad \dots(4)$$

$$v_{rx} = \sin(\theta_{rx}) / \lambda \quad \dots(5)$$

$$v_{ry} = \sin(\theta_{ry}) / \lambda \quad \dots(6)$$

For reflected angles, we have,  $\theta_{rx} = \theta_x$ ,  $\theta_{ry} = \theta_y$ ,  $v_{rx} = \sin(\theta_{rx}) / \lambda$ ,  $v_{ry} = \sin(\theta_{ry}) / \lambda$ .

### 2.2.2 Calculation of Reflection and Transmission Coefficients

To calculate the coefficients of the reflection and transmission waves, the incident polarization must be known. Scalar techniques do not inherently support polarization. Therefore, we need to apply a semi-vector theory to solve for the boundary conditions, which are required by electromagnetic theory to obtain the reflection and transmission coefficients  $R(v_x, v_y)$  and  $T(v_x, v_y)$ . Each plane wave in the frequency domain will be multiplied by these coefficients to find the reflected and transmitted ray respectively.

The reflection coefficients are found using the 4X4 matrix developed by Berreman for multilayered structure [2]. We assume reflection from a single planar interface and since the mediums are isotropic, the reflection and transmission coefficients are simply the Fresnel's coefficients [5].

Let us regard  $\theta_x$  and  $\theta_y$  to be the incident angles for TE (x-polarized) and TM (y-polarized) waves.  $n_i$  and  $n_t$  to be the refractive indices of the incident and transmitted mediums separated by the planar interface. Using Snell's law, we obtain  $\theta_{tx}$  and  $\theta_{ty}$  as the transmitted wave vector angles in y-z and x-z planes respectively, as seen in the previous section.

The reflection and transmission coefficients for transverse electric (TE) and transverse magnetic (TM) polarized waves are given by  $r_x, r_y, t_x$  and  $t_y$  respectively.

$$r_x = \frac{n_i \cos(\theta_x) - n_t \cos(\theta_{tx})}{n_i \cos(\theta_x) + n_t \cos(\theta_{tx})}, \text{ TE Reflection} \quad \dots(7)$$

$$r_y = \frac{n_i \cos(\theta_y) - n_t \cos(\theta_{ty})}{n_i \cos(\theta_y) + n_t \cos(\theta_{ty})}, \text{ TM Reflection} \quad \dots(8)$$

$$t_x = \frac{2n_i \cos(\theta_x)}{n_i \cos(\theta_x) + n_t \cos(\theta_{tx})} = 1 + r_x, \text{ TE Transmission} \quad \dots (9)$$

$$t_y = \frac{2n_i \cos(\theta_y)}{n_i \cos(\theta_y) + n_t \cos(\theta_{ty})} = n_i / n_t (1 + r_y), \text{ TM Trans} \dots (10)$$

The reflection and transmission coefficients for TE and TM polarized waves are:

$$R_{TE} = r_x^2, R_{TM} = r_y^2 \quad \dots (11)$$

$$T_{TE} = \left( \frac{n_t \cos(\theta_t)}{n_i \cos(\theta_i)} \right) t_x^2, T_{TM} = \left( \frac{n_t \cos(\theta_t)}{n_i \cos(\theta_i)} \right) t_y^2 \quad \dots (12)$$

For general linear polarization cases, we support waves with any polarization orientation angle. Let  $\theta_0$  be the orientation angle, specifying the direction of the electric field vector,  $\mathbf{E}$ , relative to the positive y-axis. Since both regions are isotropic, there is only one reflected and one transmitted wave. If we observe that the two normal modes for this system are linearly polarized waves with polarization along the x and y directions, the solutions for the transmitted and reflected wave are completely separable [4]. It can be determined that the incident, the reflected, and the transmitted wave with their electric field vectors pointing in the x-direction are self-consistent with the boundary conditions [7]. Hence, the x-polarized or the TE portion of the wave and the y-polarized or the TM portion of the wave can be considered independently and then recombined through linear superposition. As seen in the equations below, the terms are completely separable and there is no coupling of waves at the interface:

$$r = \{ [r_x \cos(\theta_0)]^2 + [r_y \sin(\theta_0)]^2 \}^{1/2} \quad \dots (13)$$

$$t = \{ [t_x \cos(\theta_0)]^2 + [t_y \sin(\theta_0)]^2 \}^{1/2} \quad \dots (14)$$

$$R = r^2 \quad \dots (15)$$

$$T = \left( \frac{n_t \cos(\theta_t)}{n_i \cos(\theta_i)} \right) t^2 \quad \dots (16)$$

From these equations we verify that the results obtained for TE ( $\theta_0 = 0^\circ$ ) and TM ( $\theta_0 = 90^\circ$ ) waves are the same as those obtained in Equations (11) and (12).

### 2.2.3 Implementation

As seen previously in our discussion of the angular spectrum technique, the inverse Fourier transform is used to

recombine the complex wavefront in the spatial domain. However, to solve for the reflected,  $U_r$ , and transmitted,  $U_t$ , complex wavefronts, the reflection and transmission coefficients must be multiplied to each of the angular frequencies as seen in the equations below:

$$U_r(x, y) = \iint A(v_x, v_y) \exp[-j2\pi(v_x x + v_y y)] R(v_x, v_y) \delta_{v_x} \delta_{v_y} \quad \dots (17)$$

$$U_t(x, y) = \iint A(v_x, v_y) \exp[-j2\pi(v_x x + v_y y)] T(v_x, v_y) \delta_{v_x} \delta_{v_y} \quad \dots (18)$$

We have proved that these equations support:

$$U_i(x, y) = U_r(x, y) + U_t(x, y) \quad \dots (19)$$

$$R + T = 1. \quad \dots (20)$$

In the case of a transmitted wave, the spatial frequencies are changed due to Snell's Law, as seen previously. In the spatial domain, it is necessary to compensate for this frequency change by remapping the corresponding spatial points.

## 3 EXAMPLE

In our first example, we demonstrate a Gaussian beam, with a spot size of 10  $\mu\text{m}$  and wavelength of 1550 nm, at the interface between two optical planes having refractive indices of 1 and 1.5, respectively. In Figure 3, we can see the incident beam, the reflected beam and the transmitted beam at the interface. Figure 3, verifies Equation (19), with peak intensity values of:  $U_i=1$ ,  $U_r=0.04$  and  $U_t=0.96$ .

In a second, more complex example, we model and simulate the air-sapphire interface found in the silicon-on-sapphire (SOS) technology [6]. The SOS process for the electrical portion of an opto-electronic multi-chip module (MCM) is growing in use. This SOS chip is bump-bonded to a bottom-emitting GaAs VCSEL/Detector chip, creating a complete MCM module, which can be used for source and detector components in short-haul optical interconnects [1]. The advantage of using a SOS process is that the sapphire substrate is transparent, allowing optical signals to pass through the substrate. An open area is left in the Si layer, creating a hole for the optical signal to pass into the sapphire substrate. A diagram of the MCM is shown in Figure 4(a), and a photograph of a detector chip taken through the sapphire is seen in Figure 4(b).

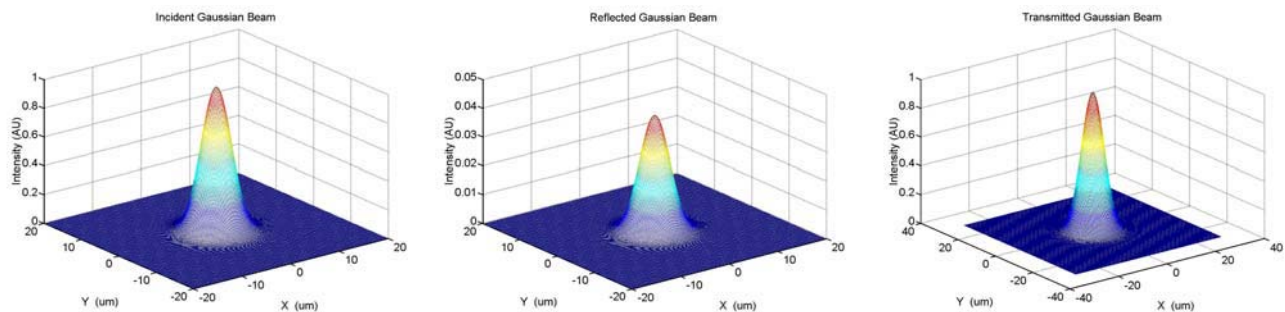


Figure 3: Incident, Reflected, and Transmitted complex optical wavefront at interface ( $n_1=1, n_2=1.5$ )

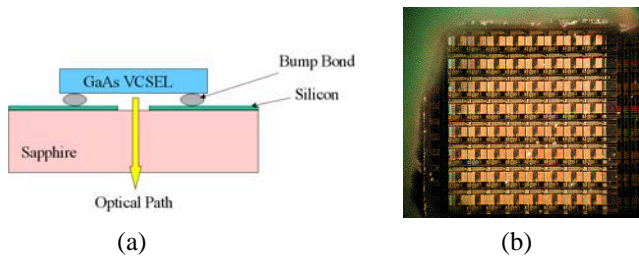


Figure 4: (a) Silicon on Sapphire (SOS) MCM  
(b) Photodetector seen through the sapphire substrate

We simulate a TE Gaussian optical wavefront, emitting from a VCSEL. The emitted Gaussian beam intensity is normalized and has a wavelength of 850 nm and a spotsize of 10  $\mu\text{m}$ . This beam is propagated 20  $\mu\text{m}$  through free-space, past the sapphire ( $n=1.77$ ) optical interface, and through 250  $\mu\text{m}$  of sapphire. Details of this system can be seen in Figure 5.

In the first stage of simulation, this beam is propagated through a free space distance of 20  $\mu\text{m}$ , which represents the gap between the GaAs VCSEL and the sapphire block. As seen in the intensity diagrams in Figure 5, the intensity drops below the normalized value of 1 with a spread in the original waist.

In the next stage, we simulate the beam propagation in the sapphire block. The reflected and transmitted Fresnel coefficients are calculated using the technique discussed in this paper. Using the reflected and transmitted Fresnel coefficients, we determine the reflected and transmitted rays at the air-sapphire interface. The transmitted ray at the interface is then propagated through a distance of 250  $\mu\text{m}$  in sapphire. Intensity plots at the different stages are shown in Figure 5.

## 4 CONCLUSION

In this paper we have presented a semi-vector technique to perform system-level simulation of optical interfaces.

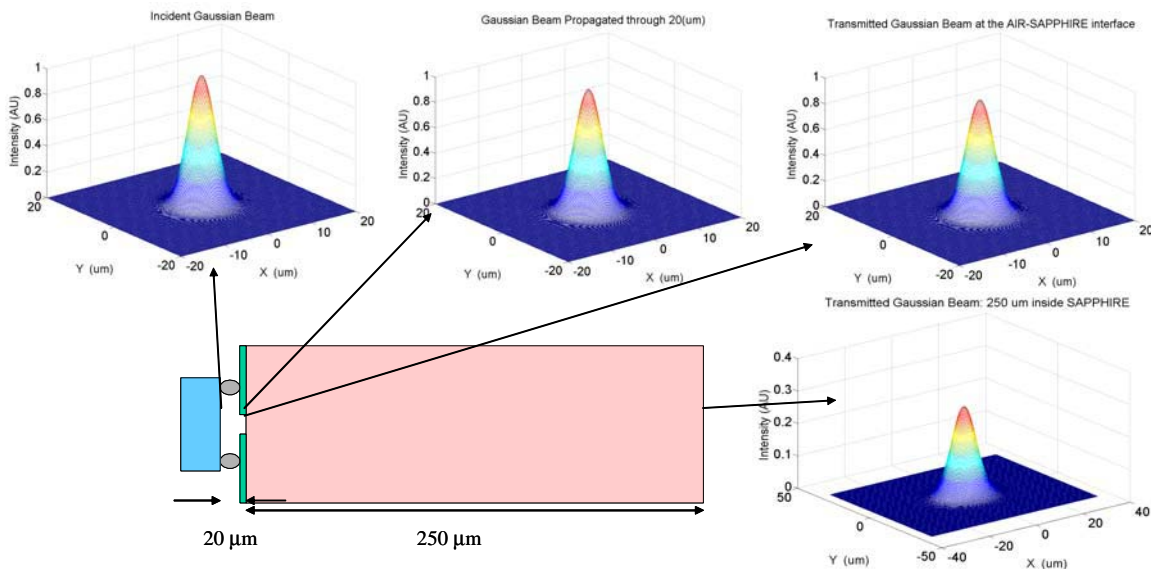


Figure 5: Simulated intensity wavefronts at stages of the Sapphire-on-Silicon MCM

This work builds on the combined advantages of using scalar methods for efficient optical propagation and vector techniques to solve for the reflection and transmission coefficients. Future work includes polarized beam propagation through complete systems and birefringent materials. Also, experimental validation of the technique will be performed for the simulated silicon-on-sapphire system.

## REFERENCES

- [1] Bakos, et. al, "Optoelectronic Multi-Chip Module Demonstrator System," OC2003, Wash., D.C.
- [2] Berreman, "Optics in stratified and anisotropic media: 4x4-Matrix formulation," J. Opt. Soc. Am., Vol 62, No.4., pp. 502-510
- [3] Kurzweg, et. al, "A Fast Optical Propagation Technique for Modeling Micro-Optical Systems," DAC, New Orleans, LA, June 10-14, 2002.
- [4] Landry, Maldonado, "Gaussian beam transmission and reflection from a general anisotropic multiplayer structure," Applied Optics, Vol. 35, No. 30, October 1996, pp. 5870-5879.
- [5] Landry, Maldonado, "Complete method to determine transmission and reflection characteristics at a planar interface between arbitrarily oriented biaxial media," J. Opt. Soc. Am. A, Vol. 12, No.9, September 1995, pp. 2048-2063.
- [6] Liu, et. al, "High bandwidth ultra thin Silicon-on-Sapphire multi-channel optical interconnects," 23 Army Conference, Session B, BP-02.
- [7] Prather, et. al "Electromagnetic analysis of finite-thickness diffractive elements," Opt. Eng. 41(8), (August 2002), pp.1792-1796.
- [8] Scarmozzino, et. al, "Comparison of finite-difference and Fourier-transform solutions of the parabolic wave equation with emphasis on integrated-optics applications," JOSA A, Vol. 8, No. 5, May 1991, pp. 725-731.